Chemical-Shift Low-Energy Photoelectron Diffraction: A Determination of the InP(110) Clean Surface Structural Relaxation

S. Gota,[1] R. Gunnella,[2] Zi-Yu Wu,[3] G. Jézéquel,[4] C. R. Natoli,[3] D. Sébilleau,[4]
E. L. Bullock,[5] F. Proix,[6] C. Guillot,[1] and A. Quémerais[4]
[1] *Laboratoire pour l'Utilisation du Rayonnement Electromagnetique, Centre Universitaire Paris-Sud, Bâtiment 209D, Orsay Cedex, France*
and SRSIM, Centre d'Etudes Nucléaires de Saclay, 91191 Gif-sur-Yvette Cedex, France
[2] *Istituto Nazionale di Fisica della Materia Research Unit, Dipartimento di Fisica, Università di Camerino, Via Madonna delle Carceri, 62032 Camerino (MC), Italy*
[3] *Istituto Nazionale di Fisica Nucleare, Laboratori Nazionali di Frascati - C. P. 13, 00044 Frascati, Italy*
[4] *Laboratoire de Spectroscopie du Solide, Université de Rennes-1, 35042 Rennes Cedex, France*
[5] *Insitut de Physique Expérimentale, Université de Lausanne, CH-1015 Lausanne-Dorigny, Switzerland*
[6] *Laboratoire de Physique des Solides, Université Pierre et Marie Curie, 75252 Paris Cedex 05, France*
(Received 2 July 1993)

We establish chemical-shift low-energy photoelectron diffraction as a novel and powerful method for the determination of clean surface structures. Combined with a new theoretical approach based on full multiple scattering theory with complex potential, the method is applied to the case of the InP(110) clean surface relaxation. The extreme sensitivity of this technique to structural parameters allows us to measure with good accuracy both the first layer and the second layer relaxation angle (respectively 23° and −5°).

PACS numbers: 79.60.Bm

A photoelectron diffraction pattern represents the modulations of the measured photocurrent, usually from a core level, as a function of the kinetic energy and/or the emission direction of the analyzed photoelectrons. As is well known, the modulations occur as the result of the interference between the primary photoelectronic wave and the portions of this wave elastically scattered by the atoms surrounding the photoabsorber. Their study therefore provides local structural information around the emitter atom [1, 2]. However, their interpretation is only simple at high photoelectron energies ($E_{\rm kin} \geq 500$ eV), where focusing effects and small scattering atomic power combine to make a simple theoretical approach work [2]. Because of the high electron mean free paths at these energies (≥ 10 Å) surface sensitivity can only be achieved when the surface atoms are of different species from the bulk ones [3] or with electrons emerging at grazing angles. For this reason few attempts at clean surface structure determination by means of x-ray photoelectron diffraction (XPD) can be found in the literature [3–5]. On the contrary, at low kinetic energies (50 to 100 eV), the photodiffraction signal from the very first layer can sometimes dominate over the bulk emission due to the concurrence of a reduced mean free path and the strong reduction of the intensity of the focusing effect, since the atomic scattering power becomes much more isotropic. For clean surfaces, where the separation of the signal from the first atomic layer from the bulk contribution is more difficult, one can further try to isolate the surface signal by exploiting the core level shift of the surface atoms with respect to the bulk ones. The price to pay for this advantage is a complication in the theoretical interpretation and analysis of the PD spectra since the scattering problem is very similar to a low-energy electron diffraction (LEED) problem. In fact atomic scattering at these energies is very strong so that the usual multiple scattering perturbation series does not converge and electron damping plays an essential role in shaping the interference patterns.

In order to test the feasibility of the "chemical shift low-energy PD" method from both an experimental and a theoretical point of view, we have studied a surface which exhibits a rather well known simple relaxation: the nonpolar InP(110) surface. There is general consensus that the main feature of this relaxation consists of outward and inward motion with respect to the ideal bulk position of the anion (P) and the cation (In), respectively. Figure 1 presents a schematic diagram of the atomic structure of the InP(110) surface in both top and side views, with indication of the rotation angles ω_1 and ω_2 for the first and second layer relaxation and the associated vertical displacements of the In and P atoms as defined in Ref. [6]. In a rigid rotation picture (i.e., bond length conservation), the angle ω_1 completely defines the relaxation. However, several groups have arrived at various structural models (e.g., addition of a small second layer relaxation ω_2 with quasiconservation of the In-P bond length) and different degrees of rotation from analysis of experimental data [7–9] and also from *ab initio* calculations [6, 10, 11].

The experiment presented in this Letter has been performed at the SuperACO storage ring at LURE, Orsay, France, on the 7° TGM monochromator of the beam line SA73. The base pressure of the analysis chamber never

0031-9007/93/71(20)/3387(4)$06.00

© 1993 The American Physical Society

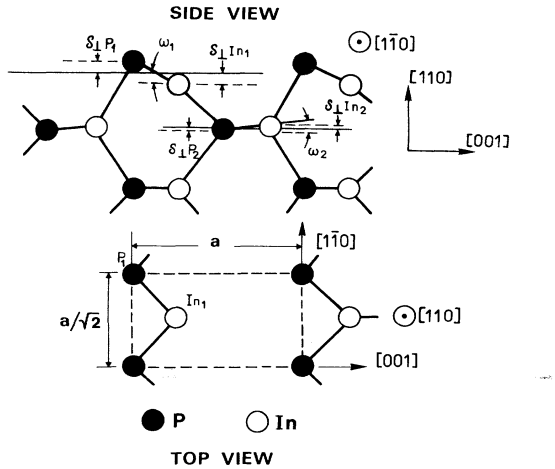

FIG. 1. Schematics of the InP(110) surface relaxation model. The top view shows the bulk extrapolated surface rectangular unit cell whereas the side view illustrates the angles ω_1 and ω_2 defining the relaxation of the first and second layers of atoms. Under this distortion the surface unit cell remains unaltered as do the atomic coordinates along the $[1\bar{1}0]$ direction.

rose above 2×10^{-10} Torr. Following standard techniques the surface was prepared by cleavage *in situ* of n-type InP bars with notches along the (110) plane. A hemispherical electrostatic electron analyzer allowing high energy and angular resolution (1°) was used. The present P $2p$ core level spectra were obtained with an overall instrumental resolution of 300 meV. Photoelectrons were excited with photons of 168 eV in order to obtain a kinetic energy corresponding to the minimum of the electron mean free path inside the solid.

The photon incidence angle with respect to the surface normal was 22.5° with the polarization vector quasiparallel to the surface plane. Electrons were collected at a fixed polar angle of 45° with respect to the surface normal corresponding to an internal emission angle of about 36° because of the refraction at the surface [1]. The azimuthal patterns were obtained by turning the sample around its normal over a range of 300°, recording the P $2p$ photoemission spectra at intervals of $\Delta\phi = 5.5°$.

In order to resolve the surface and bulk components associated to PD azimuthal patterns, a decomposition line shape analysis of the experimental P $2p$ photoemission peak in terms of two doublets corresponding to the bulk and the shifted surface spin-orbit (SO) split peaks was performed [12]. After a Shirley-type [13] background subtraction taking into account secondary electrons, the photoemission lines were modeled by Lorentzians convoluted with Gaussians to describe the effect of the core hole width and the instrumental broadening plus any additional broadening due to inhomogeneous Fermi level pinning across the surface and phonon vibrations. The same core hole width was assumed for each doublet component and for both doublets but bulk and surface Gaussian linewidths were not constrained to be equal. The observed variations in the overall shape and intensity of the raw P $2p$ peaks along the ϕ scan are to be related to the intensity variations of the surface and bulk components as a function of ϕ due to the different diffractive behavior of bulk and surface atoms [14, 15]. With this in mind the fitting of an azimuthal series was performed by keeping the same set of parameters for all the members of the series, allowing only variations of the relative intensity of the bulk and surface components in the (χ^2) optimization procedure. The following optimal parameters were found: a Lorentzian width of 0.160 eV, a SO splitting of 0.850 eV, and a surface chemical shift of 0.315 eV toward the lower binding energies very close to the starting set of parameters taken from Ref. [12]. Small variations of the order of 20% around a mean value of 0.400 eV for the Gaussian linewidth were allowed in the fit in order to account for cleavage-induced microscopic inhomogeneities of the surface. We have also allowed small variations ($\approx$ 15%) of the branching ratio between the SO split peaks around the statistical value of 2.0 for two reasons. First, the strong energy dependence of the PD patterns may influence differently the two doublet components which are separated by 0.850 eV [15, 16] and, second and more important, an azimuthal variation of the branching ratio of their intensity is expected since the excited photoelectron from each core level spin-orbit component ($2p_{1/2}$ and $2p_{3/2}$) reaches different azimuthal final states which behave differently under ϕ scan. Once the decomposition was done, the area under each doublet was normalized to the background value on the high binding energy side of the peak maximum (3 eV above). Figure 2 shows the result of the decomposition of two P $2p$ peaks recorded at two different azimuthal angles that present quite different line shapes and intensities. Figure 3 shows the normalized area of the total, surface, and bulk components as a function of the azimuthal angle. The raw data clearly showed the crystal symmetry around the $[00\bar{1}]$ direction so, in order to compensate for experimental errors the three diagrams in the figure have been mirror averaged around this direction. Discrepancies between mirror points average 8% with maximum variation of 20% giving an indication of the overall error affecting the data points. Strong anisotropies ($[I_{\max} - I_{\min}]/I_{\max}$) as high as $\approx$ 55% are observed reflecting the strong scattering regime of the photodiffraction process.

In order to interpret the azimuthal diagram of the surface PD patterns, we have applied a recently developed theoretical approach [17] based on full multiple scattering (MS) theory with complex Hedin-Lundqvist (HL) [18] potential that has been applied with success in the interpretation of x-ray absorption fine structure [19, 20]. This implies using complex atomic phase shifts as well as a complex interstitial potential [19]. It is known that the imaginary part of the HL potential reproduces quite well

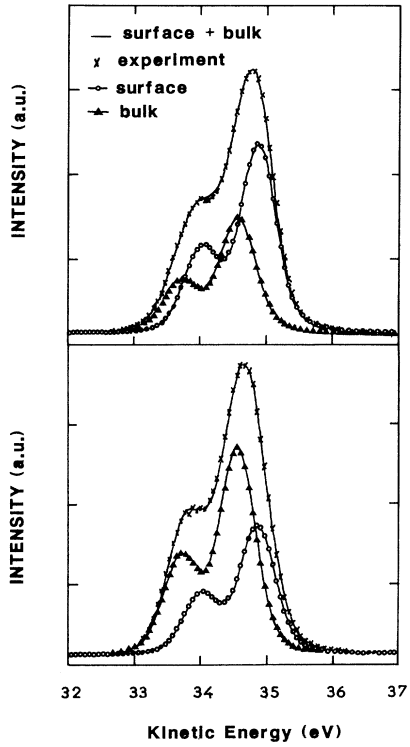

FIG. 2. Photoemission spectra of the P $2p$ core level recorded with a photon energy of $h\nu = 168$ eV and a polar angle $\theta = 45°$ at two different azimuthal angles from the InP(110) cleaved surface.

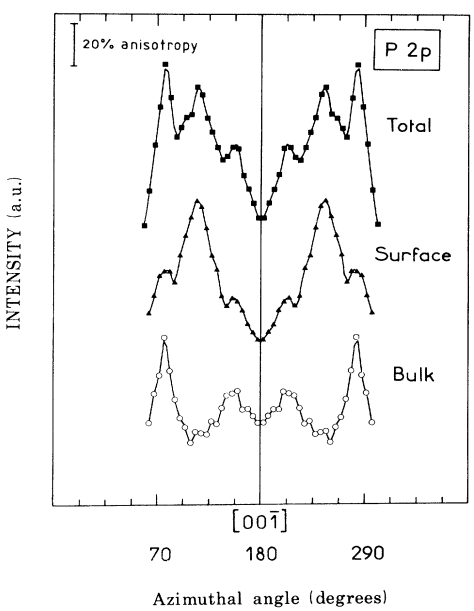

FIG. 3. Normalized area spectra of the total, surface, and bulk components as a function of the azimuthal angle. The origin of the azimuthal axis is arbitrary.

the electron mean free path in metals and semiconductors [21]. In this way the scattering amplitude centered onto the photoabsorber, whose square modulus gives the intensity of the photocurrent expected along a certain direction, has already built in the effect of the photoelectron damping in the final state and in a MS picture dies out beyond a traveled electron distance of the order of twice the electron mean free path. This means that a cluster of atoms of this radius around the photoabsorber should be sufficient to reproduce the observed PD patterns. We have therefore performed a MS muffin-tin calculation for a cluster of 59 atoms lying within a sphere of 8.44 Å. Check calculations with 85 atoms within 9.53 Å did not show any appreciable difference. Full inversion of the MS matrix was performed since for this cluster and at these photoelectron kinetic energies (≈ 45 eV) the MS series does not converge [19]. Full advantage of the symmetry point group (C_s) was taken. The construction of the charge density and potential followed the same patterns as in Ref. [19], whereas the scattering from the surface potential was taken into account only via the usual refraction condition of the exiting photoelectron through the potential step. PD patterns were calculated with an electron kinetic energy $E_{\rm kin}$ equal to the measured value of 34 eV and a real part of the muffin-tin potential $\overline{V}$ equal to 8.8 eV, implying an internal polar emission an-

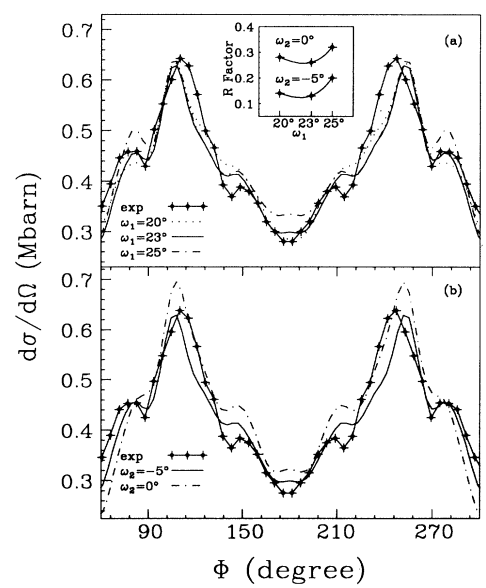

FIG. 4. (a) Comparison with experiment of different calculation at $\omega_1 = 20°$, 23°, and 25°, in the presence of a second layer relaxation angle of $\omega_2 = -5°$. The inset shows the values for the reliability factor also in the case of the absence of second layer relaxation. In both cases the calculations were performed for a kinetic energy $E_{\rm kin} = 34.0$ eV and an escape angle $\theta = 36°$. (b) Effect of the second layer counterrotation ($\omega_2 = -5°$) on the calculated spectrum with only first layer relaxation ($\omega_1 = 23°$) that best fits the data.

TABLE I. Comparison between the PD determination of the relaxation angle and the perpendicular displacement of the first and second layer P and In atoms and those from x-ray standing wave (XSW) and LEED techniques. Theoretical determinations are also reported. 1 = first layer; 2 = second layer. Distances are in Å, angles in degrees. See Fig. 1 for structural details.

Reference	$\delta_\perp P_1 \uparrow$	$\delta_\perp In_1 \downarrow$	ω_1	$\delta_\perp P_2 \downarrow$	$\delta_\perp In_2 \uparrow$
XSW, EXAFS [8]	0.180(0.1)	0.480(0.08)	27 ± 5	No sens.	No sens.
LEED [7]	0.060	0.63	30.4	0.034	0.034
This work	0.19	0.38	23 ± 3	0.07	0.06
Tot. en. min. [6]	0.176	0.467	26.5	0.041	0.073
Cluster model [10]	0.210	0.460	25.3	...	...

gle of 36°.

With these values several calculations with different surface relaxation models have been performed. First only rigid rotations of the P and In pairs in the first layer were considered with various relaxation angles $\omega_1 = 20°, 23°, 25°, 28°, 30°$. Minimization of the reliability factor R as defined by Chambers in Ref. [2] was achieved for $\omega_1 = 23°$. With this value of the relaxation angle in the first layer, a counterrotation with angle $\omega_2 = -3°, -5°, -7°$ was assumed in the second layer, the best fit being obtained for $\omega_2 = -5°$. Other relaxation models were tried, like that of Meyer *et al.* [7] obtaining worse reliability factors. Figure 4(a) compares with the experimental data different calculations for $\omega_1 = 20°, 23°, 25°$ in the presence of a second layer relaxation angle of $\omega_2 = -5°$. In the inset are shown the values of the reliability factor also in the case $\omega_2 = 0°$. Figure 4(b) indicates the effect on the calculated spectrum of the second layer counterrotation on the best fit for the first layer. A substantial improvement is obtained. It is concluded that $\omega_1 = 23° \pm 3°$. Values for the vertical displacement of the surface atoms relative to the ideal surface geometry are 0.19 Å and −0.38 Å, respectively, for P and In atoms in the first layer, in good agreement with recent x-ray standing wave analysis [8] and −0.07 Å and 0.06 Å for the same atoms in the second layer. Table I summarizes the situation for the structural relaxation found by various authors. As can be seen, good agreement is found with previous direct experimental and theoretical determinations except with the LEED method [7].

In conclusion, the combination of a chemical shift low energy photoelectron diffraction for isolating the surface contribution in the PD spectrum of a clean surface with a novel theoretical approach that finds it essential to calculate the PD scattering amplitude with a complex effective potential promises to establish a powerful technique for clean surface structure determination.

One of the authors (S.G.) gratefully acknowledges the Spanish Department of Education and Science (M.E.C.) for a research grant No. PG89 17717330. Laboratoire de Spectroscopie du Solide is URA CNRS 1202.

[1] W. F. Egelhoff, Jr., Crit. Rev. Solid St. Mater. Sci. **16**, 213 (1990).
[2] C. S. Fadley, in *Synchrotron Radiation Research: Advances in Surface Science*, edited by Z. Bachrach (Plenum Press, New York, 1990); S. A. Chambers, Adv. Phys. **40**, 357 (1991).
[3] S. A. Chambers, Surf. Sci. **261**, 48 (1992).
[4] S. Holmberg, H. C. Poon, Y. Jurget, G. Grenet, and T. M. Duc, Surf. Sci. **254**, L475 (1991).
[5] O. Knauff, U. Groshe, D. A. Wesner, and H. P. Bonzel, Surf. Sci. **277**, 132 (1992).
[6] D. J. Chadi, Phys. Rev. B **19**, 2074 (1979).
[7] R. J. Meyer, C. B. Duke, A. Paton, J. C. Tsang, J. L. Yeh, A. Kahn, and P. Mark, Phys. Rev. B **22**, 6171 (1980).
[8] J. C. Woicik, T. Kendelewicz, K. E. Miyano, P. L. Cowan, C. E. Bouldin, B. A. Karlin, P. Pianetta, and W. Spicer, Phys. Rev. Lett. **68**, 341 (1992).
[9] J. C. Woicik, T. Kendelewicz, K. E. Miyano, M. Richter, C. E. Bouldin, B. A. Karlin, P. Pianetta, and W. Spicer, Phys. Rev. B **46**, 9869 (1992).
[10] R. Chang and W. A. Goddard III, Surf. Sci. **144**, 311 (1984).
[11] C. Mailhiot, C. B. Duke, and D. J. Chadi, Surf. Sci. **149**, 366 (1985).
[12] W. G. Wilke, V. Hinkel, W. Theis, and K. Horn, Phys. Rev. B **40**, 9824 (1989).
[13] A. Shirley, Phys. Rev. B **5**, 4709 (1972).
[14] S. Gota, Thése de doctorat, Université Pierre et Marie Curie, Paris, 1993 (unpublished).
[15] L. Pattey, E. L. Bullock, and K. Hricovini, Surf. Sci. **269/270**, 28 (1992).
[16] E. L. Bullock, L. Pattey, S. Gota, K. Hricovini, and G. Jezequel (unpublished).
[17] R. Gunnella, C. R. Natoli, Z. Y. Wu, and M. Pallotta (unpublished); C. R. Natoli, M. Benfatto, C. Brouder, M. F. Ruiz López, and D. L. Foulis, Phys. Rev. B **42**, 1944 (1990).
[18] L. Hedin and S. Lundqvist, in *Solid State Physics*, edited by H. Ehrenreich *et al.* (Academic, New York, 1969), Vol. 23, p. 1; B. I. Lundqvist, Phys. Kondens. Materie **6**, 206 (1967).
[19] T. A. Tyson, K. O. Hodgson, C. R. Natoli, and M. Benfatto, Phys. Rev. B **46**, 5997 (1992).
[20] J. J. Rehr, R. C. Albers, and S. I. Zabinsky, Phys. Rev. Lett. **69**, 3397 (1992); A. Filipponi, A. Di Cicco, T. A. Tyson, and C. R. Natoli, Solid State Commun. **78**, 265 (1991); J. Mustre de Leon, J. J. Rehr, S. I. Zabinsky, and R. C. Albers, Phys. Rev. B **44**, 4146 (1991).
[21] D. R. Penn, Phys. Rev. B **35**, 482 (1987).